

Article

Not peer-reviewed version

Multi-Omics Analysis for Assessment of Hepatoprotective Activity of Nature-derived Polyphenols in Case of Non-Alcoholic Fatty Liver Disease (NAFLD) Mouse Model

[Alexander G. Brzhozovskiy](#) ^{*} , [Savva D. Semenov](#) , [Natalia V. Zakharova](#) , [Maria N. Yurova](#) , [Alexander Y. Zhrebker](#) , [Anna E. Bugrova](#) , [Oxana A. Kovaleva](#) , [Alexander L. Semenov](#) , [Dmitry P. Abroskin](#) , [Daria A. Kharina](#) , [Elena I. Fedoros](#) , [Alexey S. Kononikhin](#) , [Evgeniy N. Nikolaev](#) ^{*}

Posted Date: 15 May 2025

doi: [10.20944/preprints202505.1120.v1](https://doi.org/10.20944/preprints202505.1120.v1)

Keywords: polyphenols; hepatoprotection; mass spectrometry; biomarkers; mice



Preprints.org is a free multidisciplinary platform providing preprint service that is dedicated to making early versions of research outputs permanently available and citable. Preprints posted at Preprints.org appear in Web of Science, Crossref, Google Scholar, Scilit, Europe PMC.

Copyright: This open access article is published under a Creative Commons CC BY 4.0 license, which permit the free download, distribution, and reuse, provided that the author and preprint are cited in any reuse.

Disclaimer/Publisher's Note: The statements, opinions, and data contained in all publications are solely those of the individual author(s) and contributor(s) and not of MDPI and/or the editor(s). MDPI and/or the editor(s) disclaim responsibility for any injury to people or property resulting from any ideas, methods, instructions, or products referred to in the content.

Article

Multi-Omics Analysis for Assessment of Hepatoprotective Activity of Nature-Derived Polyphenols in Case of Non-Alcoholic Fatty Liver Disease (NAFLD) Mouse Model

Brzhozovskiy A.G.¹, Semenov S.D.^{1,3}, Zakharova N.V.², Yurova M.N.^{1,4}, Zhrebker A.Y.¹, Bugrova A.E.^{1,2}, Kovaleva O.A.¹, Semenov A.L.⁴, Abroskin D. P.¹, Kharina D. A.¹, Fedoros E.I.⁴, Kononikhin A.S.¹ and Nikolaev E.N.¹

1. Project Center of Omics Technologies and Advanced Mass Spectrometry, 121205 Moscow, Russia

2. Emanuel Institute of Biochemical Physics, Russian Academy of Science, Moscow, Russia

3. Moscow Center for Advanced Studies, 123592 Moscow, Russia

4. N.N. Petrov National Medical Research Center of Oncology, 197758 Saint Petersburg, Russia

* Correspondence: agb.imbp@gmail.com; ennikolaev@gmail.com

Abstract: The aim of this study was to examine the hepatoprotective activity of multicomponent mixtures of natural origin in the BALB/C mouse model (59 female mice), with non-alcoholic fatty liver disease (NAFLD) induced by the administration of streptozotocin (STZ) in combination with a high-fat, high-fructose diet. The hepatoprotective activity of activated hydrolytic lignin (BP-Cx-1), metanolic fraction of BP-Cx-1 (BP-Cx-M) and isoflavones from kudzu Pueraria lobata roots (IFL) was evaluated using mass spectrometry (MS)-based omics technologies. Untargeted label-free DIA quantitation resulted in 8088 protein groups identification (FDR 1%) in 40 liver tissue extracts. All treatment NAFLD groups were closer to the control samples on the liver proteomic landscape with the best results shown for BP-Cx-1-m and ISF groups. This corroborated well with metabolomic fingerprinting by FTICR MS. In order to identify differences between specific groups, we applied the post-hoc Dunn's Test and used Hedges' g as the Effect Size metric and 64 proteins that tended to return to their normal level after treatment were revealed. Pathophysiologically specific proteomics changes occurring during NAFLD were mostly associated with metabolism of the proteins (PSMD7, HCFC1) and deubiquitination pathways (UCHL3). It is worth noting that BP-Cx-1 isolated methanol fraction (Bp-Cx-m) demonstrated the pronounced increased hepatoprotective activity due to the enrichment with active components such as polyphenols. Additionally, it was shown that treatments with Bp-Cx-M and IFL significantly reduced DNA damage by 50% compared to the NAFLD untreated group. Finally, MS-based multiomics approach demonstrated its power as an advanced screening method for the assessment of the hepatoprotective activity and molecular mechanisms of action of complex multicomponent mixtures of natural origin.

Keywords: polyphenols; hepatoprotection; mass spectrometry; biomarkers; mice

1. Introduction

Non-alcoholic fatty liver disease (NAFLD), also defined as metabolic dysfunction-associated steatotic liver disease (MASLD), is a hepatic manifestation of a systemic metabolic disorder that is closely associated with obesity, insulin resistance and dyslipidemia [1–5], and is the most common cause of chronic liver disease worldwide affecting 17%–46% of Western populations and about 30% of Chinese population [5–10] with a trend towards a significant increase in the number of people at risk [10,11]. NAFLD encompasses a spectrum of conditions associated with different prognoses that can be classified into two histological forms: non-alcoholic fatty liver (NAFL) and non-alcoholic

steatohepatitis (NASH) [12,13]. The latter form is characterized by twice as rapid progression of fibrosis and covers a spectrum of liver diseases of varying severity: from inflammation and fibrosis to cirrhosis and hepatocellular carcinoma (HCC); although NASH is less common than NAFLD in general, affecting 1.5-6.5% of adults worldwide [13,14].

The pathophysiology of NAFLD involves a complex synergistic interaction of multiple factors involving cross-talk between adipose tissue, liver, pancreas and gut [13–15]. In this context, insulin resistance (IR) plays a key role in inducing hepatic de novo lipogenesis, which ultimately leads to hepatic fat deposition, increased lipotoxicity, mitochondrial dysfunction, oxidative stress, increased bowel permeability, increased free fatty acids (FFAs) circulation levels, stimulation of proinflammatory cytokine production, the formation of chronic inflammation, activation of hepatic stellate cells and deposition of a fibrous matrix [15–17]. In addition, abnormal ectopic fat deposition in organs other than the liver is associated with an increased risk of cardiovascular disease (CVD), type-II diabetes, and kidney disease, which in turn may increase the severity of NAFLD and the progression of NASH. It is noteworthy that CVD is the most common cause of death in NAFLD [13,18]. Therefore, NAFLD studies are of the same importance as CVD studies, and the high research activity in different aspects of NAFLD is highly relevant.

The use of a high-fat diet (HFD) in rodents is a popular tool for modeling obesity and metabolic disorders in NAFLD [19–21]. Inbred mouse strains provide an opportunity to both study the genetic drivers of NAFLD and identify tissue-specific signatures [22,23]. In particular, the mouse studies clarified the essential role of the gut microbiota [24–27] and its influence on the development of NAFLD independently of obesity [20]. Hepatic steatosis and its molecular signatures were studied in over 100 different inbred mouse strains of the Hybrid Mouse Diversity Panel (HMDP) fed the HFD to promote hepatic triglyceride accumulation, a hallmark of NAFLD [22]. The resulted rich multi-omics data resource, including strains with varying degrees of NAFLD, was further used in a multi-tissue integrative study and identified tissue-specific and common processes between adipose and liver tissues, and showed that knockdown of *Fasn*, *Thrsp*, *Pk1r*, and *Chchd6* genes *in vivo* improved both steatosis and insulin resistance, specifically highlighting mitochondrial dysfunction as a key driver of NAFLD [23]. Nicotine treatment particularly resulted in exacerbation of hepatic steatosis due to decreased expression of CDGSH iron sulfur domain 3 (CISD3), mitochondrial dysfunction and impaired β -oxidation; *Cisd3*-knockout increased lipid accumulation, aggravating oxidative stress and apoptosis [28]. Additionally, chronic NAFLD was shown to induce pronounced pathological features of Alzheimer's disease in both wild-type and APP transgenic mice, which were associated with neuronal apoptosis and decreased brain expression of low-density lipoprotein receptor-related protein-1 (LRP-1), indicating a link between chronic inflammation outside the brain and the induction of neurodegeneration even in the absence of genetic predisposition [29]. Also, due to the increased expression of adipocyte-specific genes detected in hepatocytes in NAFLD, as well as the disruption of the secretory function of hepatocytes, it was suggested that adipogenic changes in hepatocytes are involved in the pathogenesis of NAFLD [30].

In addition to elucidating pathophysiological mechanisms, mouse models are widely used to search for potential agents for the treatment of NAFLD. Due to the important role of the gut and microbiota in NAFLD, many studies have looked at various ways to reduce intestinal mucosal inflammation by influencing the microbiome [24,26,27]. In addition, treatment options for NAFLD have been proposed using pharmaceuticals based on bile acids, as well as a cholesterol absorption inhibitor and phytosterols that reduce the level of low-density lipoproteins in the blood plasma [31,32]. Recently, there has been increased attention to the possible therapeutic effects of plant-based ingredients. In particular, Oxymatrine (OMT), an alkaloid from *Sophora flavescens*, effectively improved liver dysfunction in diabetic mice by suppressing oxidative stress, inflammation, and fibrosis. OMT markedly increased the activity of key antioxidant enzymes and led to improvements in liver histopathology, significantly reducing the expression of NOD-like receptor protein 3 (NLRP3), interleukin-1 β (IL-1 β), transforming growth factor- β 1 (TGF- β 1), and collagen I [33]. Ganjianglingzhu decoction, a representative traditional Chinese medicine, protected against the development of lean NAFLD by regulating glucose and lipid metabolism, inhibiting the levels of sn-3-O-(geranylgeranyl) glycerol 1-phosphate and lysoPC(P-18:0/0:0) in glycerophospholipid

metabolism [34]. A polysaccharide isolated from the aqueous extract of Panacis Japonici rhizome significantly reduced liver fat accumulation and blood lipid elevation by influencing the gut microbiota: its consumption decreased the abundance of *Turicibacter*, *Dubosiella* and *Staphylococcus* and increased the abundance of *Bacteroides*, *Blautia* and *Lactobacillus* [35]. In addition, a positive effect on the gut microbiome has been shown for bound polyphenols from foxtail millet [36].

Our recent study provided strong indications of the high hepatoprotective activity of multicomponent mixtures of natural origin containing polyphenols in the BALB/C mice model with NAFLD induced by the toxin carbon tetrachloride (CCl₄) [37]. Here, using mass spectrometry based omics technologies, we studied the effects of activated hydrolytic lignin (BP-Cx-1), humic acid peloids (HA) and isoflavones from kudzu *Pueraria lobata* (IFL) roots in mouse model of NAFLD induced by HFD.

2. Results

2.1. Hepatoprotective Effect In Vivo

Hepatoprotective activity of multicomponent mixtures of natural origin were tested on non-alcoholic fatty liver disease (NAFLD) BALB/C mice in vivo models. During the experiment, severe metabolic disorders developed due to pancreatic dysfunction following the administration of streptozotocin (STZ) in combination with a high-fat, high-fructose diet. The number of deaths recorded among the test subjects was as follows: NAFLD group – 5 mice, NAFLD + BP-Cx-1 – 3 mice, NAFLD + BP-Cx-M – 4 mice, and NAFLD + IFL – 6 mice (Table S1).

From the first week until the end of the experiment, significant weight loss was observed in all groups that underwent NAFLD induction compared to the control group (Table S1). The peak weight loss occurred during the second week for all groups, after which a trend toward weight restoration was noted, particularly in the BP-Cx-M and IFL groups. However, significant differences in body weight between the NAFLD control group and the groups receiving hepatoprotection were not observed. In summary, BP-Cx-1 and BP-Cx-M were found to somewhat improve the survival of animals with induced NAFLD but did not impact the dynamics of weight loss.

Micro/macropvesicular steatosis was observed in liver sections across all experimental groups (Table S1, Figure 1). The average steatosis index in the Negative Control group was 0.22 ± 0.15 , while in the Control NAFLD group, it increased significantly to 2.43 ± 0.30 points ($p < 0.0001$). Intake of multicomponent mixtures of natural origin resulted in a reduction of the steatosis index: a 39% decrease in the IFL group (to 1.50 ± 0.22 points, $p = 0.0681$ vs. Control), a 41% decrease in the Bp-Cx-1 group (to 1.44 ± 0.18 points, $p = 0.0409$), and a 43% decrease in the Br-Cx-m group (to 1.16 ± 0.18 points, $p = 0.0147$).

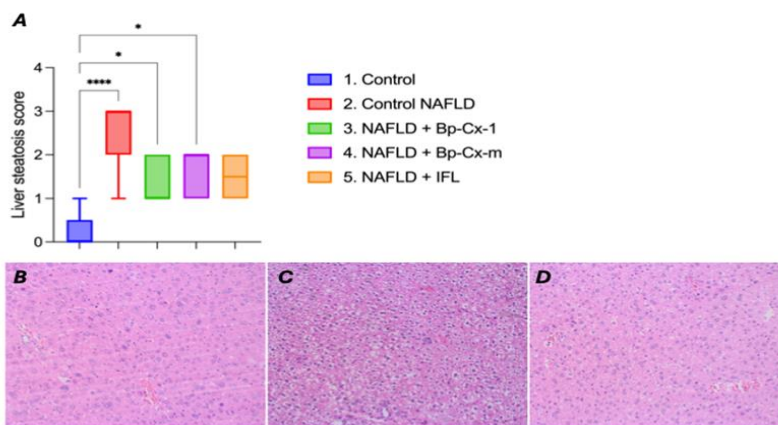


Figure 1. Hepatoprotective activity of naturally derived compounds in the NAFLD model in BALB/C mice. (A) Results of scoring liver steatosis on histological sections (Boxplot 95%CI, Kruskal-Wallis test with Dunn's correction, differences are statistically significant: *- $p < 0.05$, ***- $p < 0.0001$). Microphotographs of liver sections

(magnification x200, stained with hematoxylin and eosin): (B) Control group: 0 points; (C) NAFLD control group: 3 points; (D) NAFLD + BP-Cx-1 group: 2 points.

A significant decrease in serum albumin and globulin levels was observed in all experimental groups compared to the negative control (Table S2). The levels of aspartate aminotransferase (AST) and alanine aminotransferase (ALT) increased significantly—by 1.5 times—in the NAFLD compared to the negative control. In contrast, the intake of multicomponent mixtures of natural origin resulted in the normalization of these indicators. A similar trend was noted for both total and conjugated bilirubin levels.

A tendency for the calcium to magnesium ratio to increase was observed in the NAFLD group. In contrast, the intake of BP-Cx-M led to a significant decrease in this ratio. Additionally, the creatinine level was significantly reduced in the NAFLD, while the alkaline phosphatase content was significantly higher compared to the controls across all experimental groups.

2.2. Proteomic Analysis

Untargeted label-free quantitation (LFQ) was used to evaluate the changes in proteomic composition of liver tissue samples collected on the 35th day. As the result of proteomic analysis of 40 liver extracts 8088 protein groups were identified (FDR 1%) using DIA NN software. Initially, only those features present in 80% of the samples were selected for further analysis, resulting in 7214 features (89.19%) (Table S3). To assess the changes in the proteome composition between different treatment groups, Kruskal–Wallis test with FDR correction (FDR < 0.05) were used at a statistical significance level of q -value < 0.05, as the result 473 proteins were identified (Figure 2C). The T-SNE dimensionality reduction method shows the distribution of samples into major clusters (BP-Cx-M, BP-Cx-1 and other groups) (Figure 2A). Annotation of 473 significantly changed proteins using GO database revealed their participation in immune system pathways (68 proteins), in particular in innate immune system pathways (43 proteins) such as neutrophils degranulation (26 proteins). Several proteins were also participated in apoptosis (Bcap31, Dynll2, Fas, Gsn, Oma1, Hmgb1, Ppp3r1, Gas2, Ptk2) and response to stress (29 proteins) and chemical stress (17 proteins). Notably, some of significantly changed proteins were involved in antioxidant activity (Sod2, Ccs, Ptgs1, Fabp1, Alox5ap, Gpx1, Gpx3, Selenot, Prdx6b, Txnrd2, Gstt2) as well as oxidative stress response (Sod2, Gpx1, Gpx3, Txn2, Txnrd2, Gstt2) and redox pathway participation (Sod2, Cybb, Gclm, Txn1, Ptgs1, Gpx1, Gpx3, Prdx6b, Txnrd2, Gstt2).

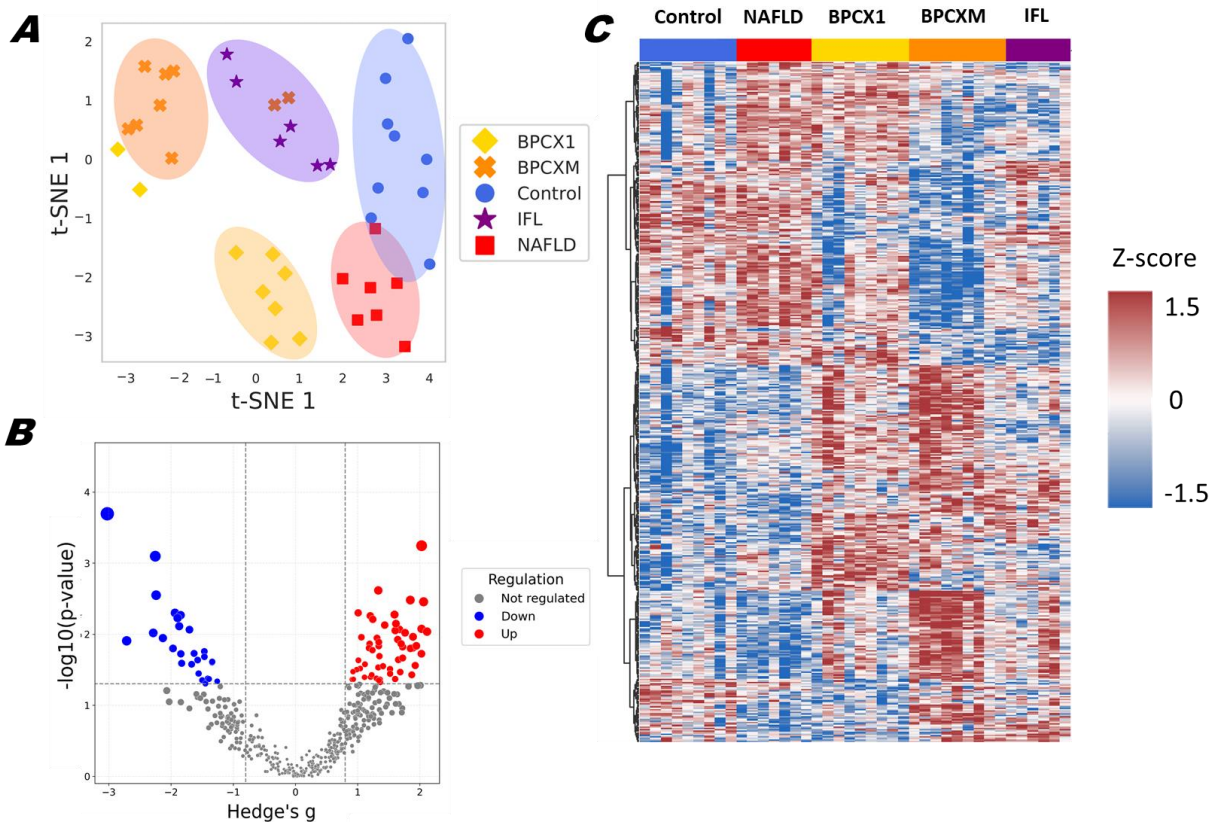


Figure 2. Liver proteomic landscape changes for Control, NAFLD and NAFLD mice groups with three types of treatment (BPCX1, BPCXM, IFL): (A) Clusterization by t-SNE of liver proteomic data for all 40 samples. Colored dots depict the liver samples: Control—red; NAFLD—blue; BPCX1—yellow; BPCXM—orange; IFL—violet. (B) Volcano plot, representing proteins significantly upregulated or downregulated in NAFLD group ($p\text{-value} < 0.05$; Hedges' g effect size > 0.8). (C) Heat map of the significantly changed liver proteins ($\text{FDR} < 0.05$) based on the z-scores of the normalized LFQ values. The strength of the colors indicates the relative abundance of the protein in different groups.

In order to identify differences between specific groups, we applied the post-hoc Dunn's Test (Table S4) and used Hedges' g as the Effect Size metric ($p\text{-value} < 0.05$; Hedges' g effect size > 0.8). Specifically, this approach allowed us to identify 83 proteins that were significantly different between the negative and positive control groups (Figure 2B). Levels of 64 of these proteins tended to return to normal with the treatments used (Figure 3). To demonstrate the strength of the treatment effect, we constructed a graph illustrating the change in the relative concentration of proteins under the treatment (Figure 3). Those proteins participate in protein metabolism (16 proteins) specifically in post-translational protein modification (13 proteins). In total, 238 proteins identified in the treatment groups were significantly different to untreated NAFLD. They include proteins participating in cellular response to stress (Atp6v1b2, Sod2, Dnajb6, Cybb, Surf1, Dynll2, Cox14, Dctn2, Txn1, Dctn3, Hspb8, Psmd8, Gpx1, Gpx3, Txn2, Lamtor3), response to chemical stress (Sod2, Cybb, Surf1, Cox14, Txn1, Psmd8, Gpx1, Gpx3, Txn2), in detoxification of reactive oxygen species (Sod2, Cybb, Txn1, Gpx1, Gpx3, Txn2) as well as Hydrogen peroxide metabolic process (Sod2, Cybb, Hbby, Gpx1, Gpx3, Prdx6b) and cell redox homeostasis (Txn1, Ero1lb, Gpx1, Txn2, Prdx6b). For an even greater number of proteins, significant differences were found relative to the both control groups in any treatment, although the control groups themselves did not differ in these proteins. Changes in levels of 106 proteins were reproducible across the different treatments used, with 65 significantly increased and 41 decreased proteins relative to the both control groups. These proteins are essentially involved in cytoplasmic ribosomal process, glutathione peroxidase activity, mitochondrial respiratory chain complex IV assembly and proton-transporting ATP synthesis, glucocorticoid biosynthesis, etc.

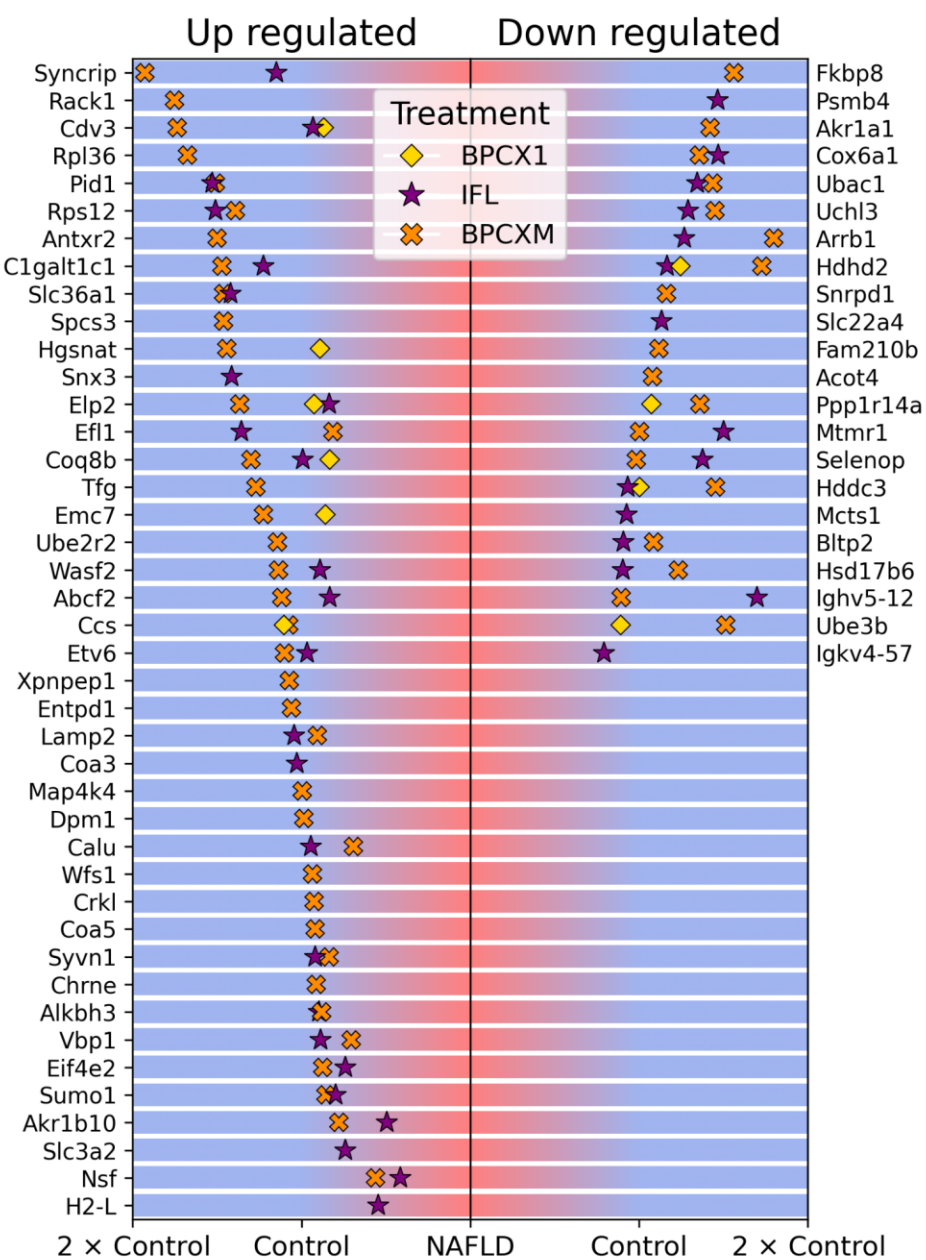


Figure 3. The effect of treatment assessment via analysis of relative concentration for differentially expressed liver tissue proteins for NAFLD mice groups in comparison to the Control group. The relative concentrations for up and down regulated proteins were calculated as described in Methods part (4.3.3 Data analysis).

2.3. Results of Molecular Fingerprinting by FT-ICR MS

While proteomic analysis enabled reliable identification of proteins connected to the oxidative stress, non-targeted metabolomic fingerprinting allows to superficially examine the effect of therapeutic agents. We applied a FTICR MS approach similar to the previously published work [37]. Numbers of molecular formulae (MF) found in at least 80% of the samples in each group were 440, 664, 689, 868 and 671 for control, NAFLD, BP-Cx-1, BP-Cx-1-M and IFL treatment, respectively. It was previously shown that BP-Cx-1 components can penetrate liver tissue therefore, it was expected to observe a significant number of unique MF in the case of these mixtures. Without metabolite identification, statistical analysis revealed a positive action of therapeutic agents used in the study. PLS-DA biplot shows a clear separation of experimental groups (Figure 4A). All treatment groups were closer to the control samples with the best results shown for BP-Cx-1-M and ISF groups. This corroborated well with the proteomic analysis.

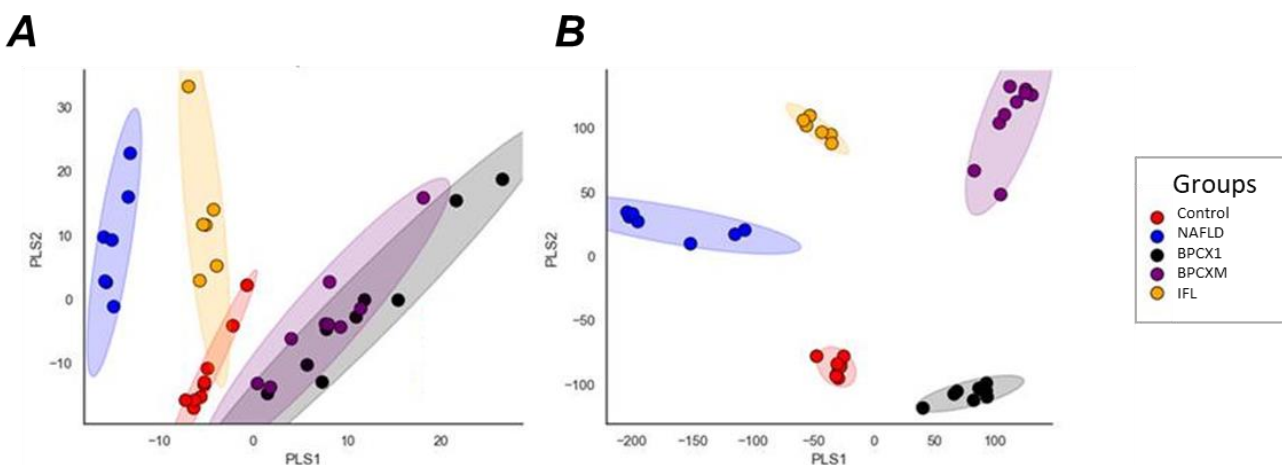


Figure 4. Results of PLS-DA analysis of FTICR MS data for PPL-extracted liver metabolites for Control, NAFLD and NAFLD mice groups with three types of treatment (BPCX1, BPCXM, IFL): A) Molecular formulae (MF) abundances, B) Normalized formulae-difference frequencies (FDS).

Previously we have shown that while direct infusion FTICR MS analysis is sensitive to carbon concentrations and to small isolation errors, the formulae-difference statistics (FDS) is more robust facilitating better inter-sample and interlaboratory comparison [38]. Application of FDS supports the results of MF-based PLS-DA analysis and indicates pronounced differences between NAFLD and control groups with positive impact of polyphenolic agents (Figure 4B). While MF-based analysis directs toward normalization of major metabolite production, FDs provides additional insights on the biochemical processes. From Figure 4B it is seen that while the relative abundance of metabolites was closer to control in ISF and especially in BP-Cx-1-m groups, BP-Cx-1 likely facilitates normalization of the whole metabolic process. It was shown recently that direct attribution of FDS to chemical reactions can be misleading [39]. Therefore, more detailed structural information on metabolites is required for in-depth annotation of FDS. Consequently, both MF and FDS analysis support the proteomic analysis but how metabolic pathways change upon administration of polyphenols remain unknown.

2.4. Evaluation of potential antigenotoxic action of nature-derived polyphenols *in vivo* study

Additionally, a study of the potential antigenotoxic action of multicomponent mixtures of natural origin was performed for the NAFLD model. The studies were performed using an alkaline version of the DNA comet assay (for the detection of single-strand breaks and alkali-labile sites or double-strand breaks).

The results of the DNA Comet assay (Figure 5) indicate a four-fold increase in DNA damage in liver cells from the NAFLD control group compared to the negative control group (8.2 ± 0.77 vs. 2.1 ± 0.27 , $p < 0.0001$). The administration of Bp-Cx-1 resulted in a slight reduction in the severity of STZ-induced damage (5.8 ± 0.61 , $p = 0.0806$ compared to group 2). In contrast, the treatments with Bp-Cx-M and IFL significantly reduced DNA damage by 50% compared to the NAFLD control group, with values of 4.2 ± 0.59 ($p = 0.0008$) and 4.4 ± 0.86 ($p = 0.0037$), respectively.

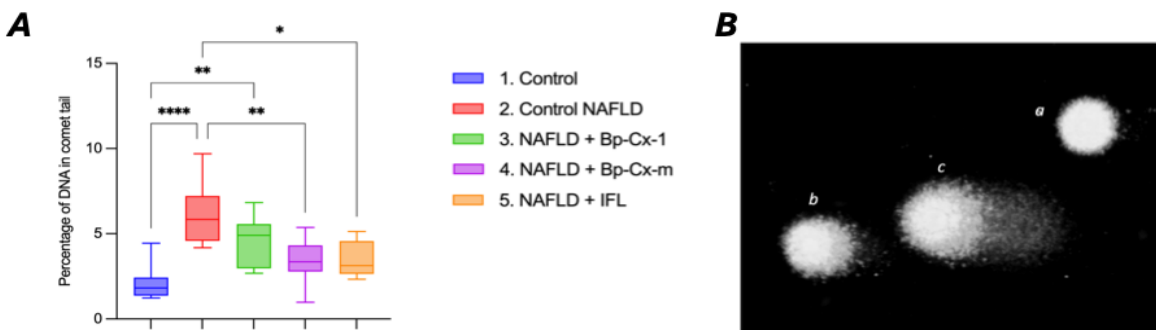


Figure 5. Results of DNA Comet Assay in liver cells for Control, NAFLD and NAFLD mice groups with three types of treatment (Bp-Cx-1, Bp-Cx-m, IFL). (A) Percentage of comet tail DNA in hepatocytes of female BALB/C mice upon NAFLD induction. Boxplot 95%CI, Kruskal-Wallis test with Dunn's correction, differences are statistically significant: *- $p<0.05$, **- $p<0.01$, ***- $p<0.0001$. (B) Micrographs of comets (magnification $\times 200$, stained with SYBR green), showing cells with intact (a) and damaged (b, c) DNA.

3. Discussion

The study conducted on a NAFLD model, induced by a combination of streptozotocin along with a high-fat and high-fructose diet, demonstrated that the examined multicomponent mixtures of natural origin have a significant hepatoprotective effect. In a previous study on the topic of hepatoprotective activity of nature-derived polyphenols we suggested that isolation of least polar fraction from BP-Cx-1 may increase its hepatoprotective activity [37]. Proteomic analysis is corroborated with molecular fingerprinting and reveals a new insight on the molecular mechanism of the hepatoprotective activity of multicomponent mixtures of natural origin. PCA analysis demonstrated a clear cluster of NAFLD and samples after treatment with nature-derived polyphenols. Changes occurring during NAFLD were mostly associated with metabolism of the proteins, notably Psmd7, Hcfc1, Uchl3 were involved in significantly changed proteins in deubiquitination pathways that are involved in the NAFLD pathophysiology [40,41]. Those proteins belong to ubiquitin C-terminal hydrolases Psmd7 play a role in removing misfolded or damaged proteins [42] and Uchl3 controls levels of cellular ubiquitin through processing of ubiquitin precursors and ubiquitinated proteins [43].

The use of BP-Cx-1, particularly the isolated methanol fraction (BP-Cx-M), increased the survival rate of experimental animals, reduced the degree of liver damage, and helped normalize the levels of AST, ALT, and bilirubin in the blood serum of the animals. Significantly changed proteins involved in the oxidant detoxification process and demonstrate a pronounced antioxidant activity (Sod2, Ccs, Ptgs1, Gpx1, Gpx3, Prdx6b, Gst2). Superoxide dismutase, mitochondrial (Sod2) responsible for the regulation of superoxide radical anion by catalyzing the dismutation of superoxide to H_2O_2 [44]. Glutathione peroxidase 1 and 3 reduce small soluble hydroperoxides such as H_2O_2 and protects cells and enzymes from oxidative damage [45,46]. The identified changes in the regulation of proteins involved in the assembly of cytochrome c oxidase (Surf1, Oma1, Cox14) and in the proton-transporting ATP synthase complex activity (Atp5d, Vdac1, Dmac2l) also indicate a significant restructuring of oxidative phosphorylation processes in mitochondria. This result is in a good agreement with the fact that mitochondrial dysfunction is a key driver of NAFLD [23], and therefore, its correction can achieve good therapeutic results. Overall, it should be emphasized that among the proteins whose regulation changes as a result of treatment, most do not differ between the control and untreated NAFLD groups. This result suggests the stimulation of compensatory mechanisms, due to which the observed hepatoprotective effect is achieved. Such changes can be associated with hepatoprotective activity of BP-Cx compounds. While the isoflavonoids did not impact the survival of the mice, they exhibited a similar hepatoprotective effect otherwise. Annotation of significantly changed proteins revealed activation of GPI-anchor biosynthesis (MPDU1, PIGW, UBE3B, PIGQ, DPM1) which correlates with results that were observed by Sun C. in mice NAFLD model [47].

Additionally, an antigenotoxic effect was observed in the studied compositions, particularly pronounced in the methanol fraction of BP-Cx and the isoflavonoids. The use of these components reduced the level of DNA damage, as indicated by a twofold decrease in the amount of DNA present in the comet tail of hepatocytes from the experimental animals.

The hepatoprotective effects of multicomponent mixtures, previously identified in an in vivo model of subacute liver damage induced by carbon tetrachloride (CCl₄), were confirmed in a model of NAFLD induced by a combination of STZ and HFFD [37]. However, the NAFLD model resulted in significant complications, including observed animal mortality and an increase in the steatosis index from 1.93 ± 0.22 (with CCl₄) to 2.43 ± 0.30 points. Additionally, both microvesicular and macrovesicular steatosis developed, whereas only microvesicular steatosis was previously recorded with CCl₄. In the CCl₄ model, a statistically significant decrease in liver damage was observed with the use of BP-Cx-1, while complete normalization of the indicator value was achieved with IFL. In the more severe NAFLD model, the significant reduction of steatosis (43%) index was observed in BP-Cx-M group.

In the subacute model using CCl₄, no significant changes in protein metabolism parameters were observed. However, there was an increase in the enzyme content, particularly for ALT. In the NAFLD model, the levels of the main protein fractions changed, and increases were noted in both ALT and AST, as well as in total and direct bilirubin. This indicated that the studied multicomponent mixtures had a normalizing effect on these parameters.

4. Materials and Methods

4.1. Chemicals

1. BP-Cx-1 – Water-soluble lignin derivative BP-Cx-1 [38] (Nobel Ltd, Saint Petersburg) - a sterile 0.42% ammonia solution (batch X0621D33). In the in vitro studies BP-Cx-1 was tested at a concentration of 0.0042% (V/V), for the in vivo studies - at a concentration of 0.42% (V/V).
2. BP-Cx-m – Methanol fraction of BP-Cx-1 (Nobel Ltd, Saint Petersburg) – 1 g of BP-Cx-1 extracted by 100 ml of MeOH for 3 hours via soxhlet extractor.
3. IFL – NADES isoflavones extract from kudzu root (*Pueraria montana var. lobata*) (Shaanxi Sheng, Xi'an, China) [48] [39]. Sample weight 0.82 g. An alcohol extract was prepared by adding ethyl alcohol in a weight ratio of 1:2, the solution was treated with ultrasound and centrifuged at 13,000 rpm to remove the sediment. The solution was evaporated and redissolved.

4.2. Animal Studies

All animal studies were carried out at the center for preclinical research of the Federal State Institution “National Medical Research Center of Oncology named after N.N. Petrov” of the Ministry of Health of the Russian Federation in accordance with the Study Protocol and standard operating procedures.

The study cohort comprised 59 female BALB/C mice obtained from the Stolbovaya branch of the FSBSI “Scientific Center for Biomedical Technologies of the Federal Medical and Biological Agency” of Russia. Before the start of the experiment, animals underwent quarantine and adaptation for 17 days. Mice were housed at a room temperature of 20–23 °C, a relative air humidity of 54–58%, and an air exchange rate of 8 volumes per hour. All animals received standard complete briquetted chow (Laboratorkorm, Moscow, Russia) and filtered water ad libitum. Mice were examined daily by the veterinarian.

Approval from the ethics committee of the Federal State Institution “National Medical Research Center of Oncology named after N.N. Petrov” of the Ministry of Health of the Russian Federation (protocol No 3 from 18 March 2024) was obtained prior to all animal-related studies. All in vivo experiments were carried out in accordance with international regulations (Directive 2010/63/EU of the European Parliament and of the Council of 22 September 2010 on the protection of animals used for scientific purposes).

4.2.1. Experimental Design

Mice were randomized by weight into the Negative control group (n=9) and Experimental (n=50) cohort.

In vivo model of Non-Alcoholic Fatty Liver Disease (NAFLD) in mice of experimental cohort was induced by single intraperitoneal injection of Streptozotocin (STZ) (75% α -anomer, 98% HPLC, CarboSynth, USA) at a dose of 100 mg/kg followed by high-fat and high-fructose diet (HFFD, pork fat added to a standard chow and 30% fructose solution instead of drinking water in free access) throughout the study. In 3 days after STZ injection blood samples from the tail vein were collected for glucose level measurement by a blood glucose meter (Accucheck Active, Germany) and mice were randomized by results into following groups:

1. Control—negative control—intragastric administration of placebo (drinking water) (0.2 mL/mouse) daily for 24 days (n=9).
2. Control NAFLD—positive control—intragastric administration of placebo (0.2 mL/mouse) daily for 24 days (n=12).
3. NAFLD + Bp-Cx-1—intragastric administration of Bp-Cx-1 at a dose of 80 mg/kg (0.2 mL/mouse) daily for 24 days (n=13).
4. NAFLD + Bp-Cx-M—intragastric administration of Bp-Cx-methanol at a dose of 80 mg/kg (0.2 mL/mouse) daily for 24 days (n=13).
5. NAFLD + IFL— intragastric administration of NADES isoflavones extract from kudzu root at a dose of 80 mg/kg (0.2 mL/mouse) daily for 24 days (n=12).

Body weighing was carried out once a week during experiments and prior to euthanasia.

Blood sampling was performed prior euthanasia from the tail vein: whole blood samples were collected in 2 ml Eppendorf tubes, centrifuged (10 min, 12000g) and serum samples were immediately frozen in liquid nitrogen (-196 C) and stored at -80°C. Biochemical parameters in blood serum (ALT, AST, bilirubin, creatinine, urea, total protein, albumin, globulin) were evaluated with Konelab 20 biochemical analyzer (Thermo Fisher Scientific, USA) using commercial KliniTest kits (ROO "SPbOE", Russia).

Euthanasia by CO₂ was carried out on the 27th day after STZ administration. All animals were autopsied. Liver was excised and weighted, mass index (percentage ratio of liver mass to body weight) was calculated. Two liver samples from each animal were isolated: one sample was immediately used for DNA-Comet assay, another was transferred in Eppendorf tube, frozen in liquid nitrogen and kept frozen at-80 for further analysis. The rest was histologically examined after routine histological preparation (dehydration, impregnation with paraffin, cutting into sections, staining with hematoxylin and eosin). Evaluation of liver steatosis was carried out microscopically in 10 fields (x200) per slide by a semi-quantitative method (in points): 0 – no changes, 1 – up to 30% of hepatocytes contain lipid vacuoles in the cytoplasm, 2 – 30–60% of cells are changed, 3 – more than 60% of cells are changed. Mean steatosis index was calculated per animal and onward per group.

4.2.2. DNA Comet Assay

Liver sample (50–200 mg) was isolated during autopsy, washed from blood cells, grinded, and a cell suspension was prepared in 1.5 ml of cooled buffer (20 mM EDTA-Na₂, 10% DMSO, pH 7.5). A cell suspension in agarose (1:10) was immediately prepared and applied to pre-prepared gel slides with an agarose backing. Routine processing was then performed [49], including lysis, alkaline denaturation, electrophoresis, fixation, staining (with SYBR Green dye), and microscopic analysis using a microscope with a BLB-L fluorescent module (LOMO-MA LLC, Russia). Images were digitized using an MS-20 camera (LOMO-MA LLC, Russia) and processed using Image J (Open Comet plugin). At least 100 comets were evaluated on each slide at x200 magnification, and the average % DNA in the comet tail was calculated.

4.3. Proteomic Analysis

4.3.1. Liver Samples Preparation

Liver tissue (10-20 mg) was ground into a fine powder in liquid nitrogen. Cell lysis was conducted by adding 50 mM Tris-HCl pH 8.0.150 mM NaCl, 0.1% SDS, 0.5% Na deoxycholate, 1% NP-40 lysis buffer containing a cocktail of protease inhibitors (Roche). Tissues were incubated for 30

minutes and sonicated in an ultrasonic bath twice for 3 minutes. Samples were centrifuged at 40C at 10000 g for 10 min, the supernatant was collected, and the sediment was re-extracted with denaturing buffer (8 M urea, 2 M thiourea, 50 mM Tris-HCl pH8.0, 0.5% NP-40). The supernatant was collected and pooled after the centrifugation at 40C at 10000g for 10 minutes. Protein concentration was measured by the Bradford method. 100 µg of protein was taken and precipitated with ice-cold acetone. Samples were denatured and reduced by incubation with 8 M urea, 0.1 M dithiothreitol and 100 mM Tris × HCl (pH 8.0, +37 °C, 30 min). Next, the proteins were alkylated by a 30-min incubation in the dark with 20 mM iodoacetamide. For trypsinolysis, the samples were diluted with 100 mM Tris × HCl (pH 8.0) until <1 M urea; L-(tosylamido-2-phenyl) ethyl chloromethyl ketone (TPCK)-treated trypsin (Worthington) was added at a 25:1 (protein:enzyme, w/w) ratio; and the samples were incubated for 16 h at 37 °C. The reaction was quenched by acidifying the samples with formic acid (FA) to a final concentration of 1.0% (pH ≤ 2). The resulting peptides were purified by solid-phase extraction on C18 cartridges (Oasis, Waters, USA), then lyophilized and dissolved for analysis in 0.1% formic acid.

4.3.2. LC-MS/MS Analysis

Tissue tryptic peptide LC separations were performed at a flow of 400 nL/min using a 90 min linear gradient from 2% to 37% solvent B, followed by an LC column wash step (10 min isocratic with 90% solvent B) and equilibration (15 min, isocratic, with 2% solvent B) in three technical replicates. The MS data were acquired using the diaPASEF method. Electrospray source (ESI) settings were as follows: capillary voltage 1400 V, dry gas flow - 3.0 L/min at a temperature of 180°C. The MS and MS/MS spectra were acquired from 100 to 1700 m, an ion mobility range of 0.6–1.6 1/K0 (V s/cm²). The ion mobility was scanned from 0.6 to 1.6 Vs/cm². The ramp time was set to 100 ms. The collision energy was ramped linearly as a function of the mobility from 59 eV at 1/K0 = 1.6 Vs/cm² to 20 eV at 1/K0 = 0.6 Vs/cm².

4.3.3. Data Analysis

The obtained LC-MS/MS raw data were analyzed using DIA NN (Data-Independent Acquisition by Neural Networks) software (version 1.8.1) [50] in library free mode using the following parameters: mass accuracy – 20 ppm; MS1 accuracy – 20 ppm; peptides length range 7 – 30 amino acids long was conducted across SwissProt Human database with carbamidomethylation (C), oxidation (M) as possible modifications. FDR thresholds were set to 0.1%.

The statistical analysis and data visualization were performed by Python (3.7.3) with the following packages: SciPy [51], Seaborn [52], Matplotlib [53] and Pandas [54]. A Shapiro-Wilk normality test was used for each protein and each group separately. The Benjamini–Hochberg procedure was used to control the false discovery rate (FDR). As a result, we confirmed that the assumption of data normality could be accepted at the significance level q-value < 0.05. Kruskal–Wallis test with FDR correction was used to identify potential markers between groups as well as the post-hoc Dunn's Test. To increase the test's power and control the Type I error rate, we considered results statistically significant when p-value < 0.05 and |Effect Size| > 0.8. Given the small sample size and the normal distribution of the data, we used Hedges' g as the Effect Size metric. Missing values were imputed using the k-nearest neighbors method from the FancyImpute library [55], applied separately to each feature and group.

To calculate the relative concentration for Figure 3, we used the following formula: $RC_{\{T\}} = (C_{\{T\}} - \min(C_{\{C\}}, C_{\{D\}})) / (|C_{\{C\}} - C_{\{D\}}|)$, where: $C_{\{T\}}$ - mean of the protein concentration in the treatment group T; $C_{\{C\}}$ - mean of the protein concentration in the control group; $C_{\{D\}}$ - mean of the protein concentration in the NADFL group.

4.4. Molecular Fingerprinting by FTICR

4.4.1. Extraction of Metabolites

For metabolites analysis a chloroform-methanol extraction method was used [56]. Samples were mixed with chloroform-methanol (1:2) mixture and incubated for 30 minutes with constant stirring, after that samples were sonicated twice in an ultrasonic bath. Next, water and chloroform were added

up to ratio 1/2/0.8 and centrifuged at 3000 rpm. Upper water-methanol phase was evaporated via centrifugal vacuum evaporator and purified using PPL cartridges. Metabolites were eluted with 1.5 mL of MeOH.

4.4.2. FTICR MS Analysis

Mass spectrometric analysis of metabolites was carried out using a FT-ICR MS Apex Ultra device (Bruker Daltonics), with harmonized cell equipped with a 7 T superconducting magnet and electrospray (ESI) ionization source. All mass spectra were acquired in negative ionization mode by direct infusion at flow rate 90 mL/h. The electrospray source (ESI) settings were as follows: capillary voltage - 3500 V, dry gas flow -3 (N2) l/min at a temperature of 200° C. Measurements were carried out in the mass/charge (m/z) range from 200 to 1000. Spectra were acquired at 400,000 resolutions (at m/z 400), with 250 scans accumulated for each spectrum.

4.4.3. Data Analysis

Raw FTICR MS data were treated using open-source software and lab-written Python scripts. Visualization of data has been performed with Python library Matplotlib [53]. Statistical analysis has been performed with Python libraries NumPy, Pandas and Seaborn. All *.raw files were converted to *.mzML format using msconvert with continuous wavelet transform algorithm to extract peaks with S/N >3 [57]. Peak lists were extracted using Python script based on pyteomics library [58]. Formulae assignment for all samples was conducted with python script based on open-source NOMspectra python library [59] with a denoising step adapted from Zielinski et al [60] using the following constraints: O/C ratio ≤ 1 , $0.3 < \text{H/C ratio} < 2.5$; element counts $[1 < \text{C} \leq 60, 2 < \text{H} \leq 100, 0 < \text{O} \leq 60, \text{N} \leq 3, \text{S} \leq 1]$; $z = -1$ and mass accuracy window <1 ppm after build-in internal calibration based on the construction of the probability density of assignments [61]. Only molecular assignments which presented in at least 80% of samples in each group were retained for statistical analysis. This step aimed to decrease the uncertainty of qualitative comparison raised from the unknown mass balance. High-resolution mass spectrometry data classification based on the differences in the number of elements between each pair of molecular formulae within the formulae list was conducted using open source software nommass.com [38] followed by normalization of formulae-difference frequencies (FDS) using routine python script.

5. Conclusions

Bp-Cx-M demonstrated the pronounced increased hepatoprotective activity due to the enrichment with active components such as polyphenols. Additionally, it was shown that treatments with Bp-Cx-M and IFL significantly reduced DNA damage by 50% compared to the NAFLD untreated group. Finally, MS-based multiomics approach demonstrated its power as an advanced screening method for the assessment of the hepatoprotective activity and molecular mechanisms of action of complex multicomponent mixtures of natural origin.

Data Availability Statement: Data are contained within the Supplementary Materials.

Institutional Review Board Statement: Approval from the ethics committee of the Federal State Institution "National Medical Research Center of Oncology named after N.N. Petrov" of the Ministry of Health of Russian Federation (protocol № 3 from 18.03.2024) was obtained prior to all animal-related studies. All in vivo experiments were carried out in accordance with international regulations (Directive 2010/63/EU of the European Parliament and of the Council of 22 September 2010 on the protection of animals used for scientific purposes).

Conflicts of Interest: The authors declare no conflicts of interest.

Funding: The work was carried out within the framework of the Russian Science Foundation grant No. 22-75-10140 dated (07/28/2022).

References

1. de Alwis, N.M.W.; Day, C.P. Non-Alcoholic Fatty Liver Disease: The Mist Gradually Clears. *J. Hepatol.* 2008, 48 Suppl 1, S104–12, doi:10.1016/j.jhep.2008.01.009.
2. Yang, J.; Tian, C.; Liu, M.; Guo, H.; Lin, F.; Ding, Y.; Yao, W.; Zhang, J.; Fan, J.; Yu, C.; et al. Genetic Risk, BMI Status, BMI Change Patterns, and the Risk of Steatotic Liver Disease and Liver Enzyme Elevation in Chinese Adults. *Nutrients* 2024, 16, doi:10.3390/nu16234212.
3. Tilg, H.; Effenberger, M. From NAFLD to MAFLD: When Pathophysiology Succeeds. *Nat. Rev. Gastroenterol. Hepatol.* 2020, 17, 387–388, doi:10.1038/s41575-020-0316-6.
4. Eslam, M.; Newsome, P.N.; Sarin, S.K.; Anstee, Q.M.; Targher, G.; Romero-Gomez, M.; Zelber-Sagi, S.; Wai-Sun Wong, V.; Dufour, J.-F.; Schattenberg, J.M.; et al. A New Definition for Metabolic Dysfunction-Associated Fatty Liver Disease: An International Expert Consensus Statement. *J. Hepatol.* 2020, 73, 202–209, doi:10.1016/j.jhep.2020.03.039.
5. Marchesini, G.; Bugianesi, E.; Forlani, G.; Cerrelli, F.; Lenzi, M.; Manini, R.; Natale, S.; Vanni, E.; Villanova, N.; Melchionda, N.; et al. Nonalcoholic Fatty Liver, Steatohepatitis, and the Metabolic Syndrome. *Hepatology* 2003, 37, 917–923, doi:10.1053/jhep.2003.50161.
6. Ando, Y.; Jou, J.H. Nonalcoholic Fatty Liver Disease and Recent Guideline Updates. *Clin. liver Dis.* 2021, 17, 23–28, doi:10.1002/cld.1045.
7. Vernon, G.; Baranova, A.; Younossi, Z.M. Systematic Review: The Epidemiology and Natural History of Non-Alcoholic Fatty Liver Disease and Non-Alcoholic Steatohepatitis in Adults. *Aliment. Pharmacol. Ther.* 2011, 34, 274–285, doi:10.1111/j.1365-2036.2011.04724.x.
8. Younossi, Z.M.; Blissett, D.; Blissett, R.; Henry, L.; Stepanova, M.; Younossi, Y.; Racila, A.; Hunt, S.; Beckerman, R. The Economic and Clinical Burden of Nonalcoholic Fatty Liver Disease in the United States and Europe. *Hepatology* 2016, 64, 1577–1586, doi:10.1002/hep.28785.
9. Powell, E.E.; Wong, V.W.-S.; Rinella, M. Non-Alcoholic Fatty Liver Disease. *Lancet (London, England)* 2021, 397, 2212–2224, doi:10.1016/S0140-6736(20)32511-3.
10. Hutchison, A.L.; Tavaglione, F.; Romeo, S.; Charlton, M. Endocrine Aspects of Metabolic Dysfunction-Associated Steatotic Liver Disease (MASLD): Beyond Insulin Resistance. *J. Hepatol.* 2023, 79, 1524–1541, doi:10.1016/j.jhep.2023.08.030.
11. Younossi, Z.M.; Stepanova, M.; Afendy, M.; Fang, Y.; Younossi, Y.; Mir, H.; Srishord, M. Changes in the Prevalence of the Most Common Causes of Chronic Liver Diseases in the United States from 1988 to 2008. *Clin. Gastroenterol. Hepatol. Off. Clin. Pract. J. Am. Gastroenterol. Assoc.* 2011, 9, 524–530.e1; quiz e60, doi:10.1016/j.cgh.2011.03.020.
12. Chalasani, N.; Younossi, Z.; Lavine, J.E.; Charlton, M.; Cusi, K.; Rinella, M.; Harrison, S.A.; Brunt, E.M.; Sanyal, A.J. The Diagnosis and Management of Nonalcoholic Fatty Liver Disease: Practice Guidance from the American Association for the Study of Liver Diseases. *Hepatology* 2018, 67, 328–357, doi:10.1002/hep.29367.
13. Martinou, E.; Pericleous, M.; Stefanova, I.; Kaur, V.; Angelidi, A.M. Diagnostic Modalities of Non-Alcoholic Fatty Liver Disease: From Biochemical Biomarkers to Multi-Omics Non-Invasive Approaches. *Diagnostics (Basel, Switzerland)* 2022, 12, doi:10.3390/diagnostics12020407.
14. EASL-EASD-EASO Clinical Practice Guidelines for the Management of Non-Alcoholic Fatty Liver Disease. *J. Hepatol.* 2016, 64, 1388–1402, doi:10.1016/j.jhep.2015.11.004.
15. Buzzetti, E.; Pinzani, M.; Tsouchatzis, E.A. The Multiple-Hit Pathogenesis of Non-Alcoholic Fatty Liver Disease (NAFLD). *Metabolism* 2016, 65, 1038–1048, doi:10.1016/j.metabol.2015.12.012.
16. Cusi, K. Role of Insulin Resistance and Lipotoxicity in Non-Alcoholic Steatohepatitis. *Clin. Liver Dis.* 2009, 13, 545–563, doi:10.1016/j.cld.2009.07.009.
17. Manne, V.; Handa, P.; Kowdley, K. V Pathophysiology of Nonalcoholic Fatty Liver Disease/Nonalcoholic Steatohepatitis. *Clin. Liver Dis.* 2018, 22, 23–37, doi:10.1016/j.cld.2017.08.007.
18. Després, J.-P. Body Fat Distribution and Risk of Cardiovascular Disease: An Update. *Circulation* 2012, 126, 1301–1313, doi:10.1161/CIRCULATIONAHA.111.067264.
19. Rabot, S.; Membrez, M.; Bruneau, A.; Gérard, P.; Harach, T.; Moser, M.; Raymond, F.; Mansourian, R.; Chou, C.J. Germ-Free C57BL/6J Mice Are Resistant to High-Fat-Diet-Induced Insulin Resistance and Have

Altered Cholesterol Metabolism. *FASEB J.* Off. Publ. Fed. Am. Soc. Exp. Biol. 2010, 24, 4948–4959, doi:10.1096/fj.10-164921.

20. Le Roy, T.; Llopis, M.; Lepage, P.; Bruneau, A.; Rabot, S.; Bevilacqua, C.; Martin, P.; Philippe, C.; Walker, F.; Bado, A.; et al. Intestinal Microbiota Determines Development of Non-Alcoholic Fatty Liver Disease in Mice. *Gut* 2013, 62, 1787–1794, doi:10.1136/gutjnl-2012-303816.

21. Velázquez, K.T.; Enos, R.T.; Bader, J.E.; Sougiannis, A.T.; Carson, M.S.; Chatzistamou, I.; Carson, J.A.; Nagarkatti, P.S.; Nagarkatti, M.; Murphy, E.A. Prolonged High-Fat-Diet Feeding Promotes Non-Alcoholic Fatty Liver Disease and Alters Gut Microbiota in Mice. *World J. Hepatol.* 2019, 11, 619–637, doi:10.4254/wjh.v11.i8.619.

22. Hui, S.T.; Parks, B.W.; Org, E.; Norheim, F.; Che, N.; Pan, C.; Castellani, L.W.; Charugundla, S.; Dirks, D.L.; Psychogios, N.; et al. The Genetic Architecture of NAFLD among Inbred Strains of Mice. *eLife* 2015, 4, e05607, doi:10.7554/eLife.05607.

23. Chella Krishnan, K.; Kurt, Z.; Barrere-Cain, R.; Sabir, S.; Das, A.; Floyd, R.; Vergnes, L.; Zhao, Y.; Che, N.; Charugundla, S.; et al. Integration of Multi-Omics Data from Mouse Diversity Panel Highlights Mitochondrial Dysfunction in Non-Alcoholic Fatty Liver Disease. *Cell Syst.* 2018, 6, 103–115.e7, doi:10.1016/j.cels.2017.12.006.

24. Ritze, Y.; Bárdos, G.; Claus, A.; Ehrmann, V.; Bergheim, I.; Schwierz, A.; Bischoff, S.C. *Lactobacillus Rhamnosus* GG Protects against Non-Alcoholic Fatty Liver Disease in Mice. *PLoS One* 2014, 9, e80169, doi:10.1371/journal.pone.0080169.

25. Bäckhed, F.; Ding, H.; Wang, T.; Hooper, L.V.; Koh, G.Y.; Nagy, A.; Semenkovich, C.F.; Gordon, J.I. The Gut Microbiota as an Environmental Factor That Regulates Fat Storage. *Proc. Natl. Acad. Sci. U. S. A.* 2004, 101, 15718–15723, doi:10.1073/pnas.0407076101.

26. Chen, D.; Wang, Y.; Yang, J.; Ou, W.; Lin, G.; Zeng, Z.; Lu, X.; Chen, Z.; Zou, L.; Tian, Y.; et al. Shenling Baizhu San Ameliorates Non-Alcoholic Fatty Liver Disease in Mice by Modulating Gut Microbiota and Metabolites. *Front. Pharmacol.* 2024, 15, 1343755, doi:10.3389/fphar.2024.1343755.

27. Kim, H.-J.; Jeon, H.-J.; Kim, D.-G.; Kim, J.-Y.; Shim, J.-J.; Lee, J.-H. *Lacticaseibacillus Paracasei* HY7207 Alleviates Hepatic Steatosis, Inflammation, and Liver Fibrosis in Mice with Non-Alcoholic Fatty Liver Disease. *Int. J. Mol. Sci.* 2024, 25, doi:10.3390/ijms25189870.

28. Wei, Y.; Pan, T.; Zhao, Y.; Chen, Z.; Wu, L.; Fang, S.; Wang, X.; Wang, X.; Chen, D.; Chen, Y. Nicotine Aggravates High-Fat Diet-Induced Non-Alcoholic Fatty Liver Disease in Mice via Inhibition of CISD3. *Int. Immunopharmacol.* 2024, 142, 113067, doi:10.1016/j.intimp.2024.113067.

29. Kim, D.-G.; Krenz, A.; Toussaint, L.E.; Maurer, K.J.; Robinson, S.-A.; Yan, A.; Torres, L.; Bynoe, M.S. Non-Alcoholic Fatty Liver Disease Induces Signs of Alzheimer’s Disease (AD) in Wild-Type Mice and Accelerates Pathological Signs of AD in an AD Model. *J. Neuroinflammation* 2016, 13, 1, doi:10.1186/s12974-015-0467-5.

30. Pan, X.; Wang, P.; Luo, J.; Wang, Z.; Song, Y.; Ye, J.; Hou, X. Adipogenic Changes of Hepatocytes in a High-Fat Diet-Induced Fatty Liver Mice Model and Non-Alcoholic Fatty Liver Disease Patients. *Endocrine* 2015, 48, 834–847, doi:10.1007/s12020-014-0384-x.

31. Wang, W.; Zhao, J.; Gui, W.; Sun, D.; Dai, H.; Xiao, L.; Chu, H.; Du, F.; Zhu, Q.; Schnabl, B.; et al. Tauroursodeoxycholic Acid Inhibits Intestinal Inflammation and Barrier Disruption in Mice with Non-Alcoholic Fatty Liver Disease. *Br. J. Pharmacol.* 2018, 175, 469–484, doi:10.1111/bph.14095.

32. Zheng, S.; Hoos, L.; Cook, J.; Tetzloff, G.; Davis, H.J.; van Heek, M.; Hwa, J.J. Ezetimibe Improves High Fat and Cholesterol Diet-Induced Non-Alcoholic Fatty Liver Disease in Mice. *Eur. J. Pharmacol.* 2008, 584, 118–124, doi:10.1016/j.ejphar.2008.01.045.

33. Lou, D.; Fang, Q.; He, Y.; Ma, R.; Wang, X.; Li, H.; Qi, M. Oxymatrine Alleviates High-Fat Diet/Streptozotocin-Induced Non-Alcoholic Fatty Liver Disease in C57BL/6J Mice by Modulating Oxidative Stress, Inflammation and Fibrosis. *Biomed. Pharmacother.* 2024, 174, 116491, doi:10.1016/j.biopha.2024.116491.

34. Tang, N.; Ji, L.; Shi, X.; Xiong, Y.; Xiong, X.; Zhao, H.; Song, H.; Wang, J.; Zhang, L.; You, S.; et al. Effects of Ganjianglingzhu Decoction on Lean Non-Alcoholic Fatty Liver Disease in Mice Based on Untargeted Metabolomics. *Pharmaceuticals (Basel)*. 2024, 17, doi:10.3390/ph17040502.

35. Wu, Y.; Yin, W.; Hao, P.; Chen, Y.; Yu, L.; Yu, X.; Wu, Y.; Li, X.; Wang, W.; Zhou, H.; et al. Polysaccharide from Panax Japonicus C.A. Mey Prevents Non-Alcoholic Fatty Liver Disease Development Based on Regulating Liver Metabolism and Gut Microbiota in Mice. *Int. J. Biol. Macromol.* 2024, 260, 129430, doi:10.1016/j.ijbiomac.2024.129430.

36. Ghani, I.; An, Y.; Qiao, Q.; He, S.; Li, Z. Polyphenols from Foxtail Millet Improve Non-Alcoholic Fatty Liver Disease by Regulating Intestinal Microbiome in Mice. *Foods* (Basel, Switzerland) 2024, 13, doi:10.3390/foods13111683.

37. Brzhozovskiy, A.G.; Semenov, S.D.; Zhrebker, A.Y.; Bugrova, A.E.; Yurova, M.N.; Zhernov, Y. V.; Kovaleva, O.A.; Semenov, A.L.; Abroskin, D.P.; Kruglov, S.S.; et al. Hepatoprotective Activity of Nature-Derived Polyphenols Studied by Mass Spectrometry Based Multi-OMICS Approach. *Int. J. Mol. Sci.* 2025, 26, doi:10.3390/ijms26041604.

38. Sarycheva, A.; Perminova, I. V.; Nikolaev, E.N.; Zhrebker, A. Formulae Differences Commence a Database for Interlaboratory Studies of Natural Organic Matter. *Environ. Sci. Technol.* 2023, 57, 6238–6247, doi:10.1021/acs.est.2c08002.

39. Zhrebker, A.; Babcock, O.; Pereira, D.L.; D'Aronco, S.; Filippi, D.; Soldà, L.; Michoud, V.; Gratien, A.; Cirtog, M.; Cantrell, C.; et al. Decreasing the Uncertainty in the Comparison of Molecular Fingerprints of Organic Aerosols with H/D Exchange Mass Spectrometry. *Environ. Sci. Technol.* 2024, 58, 20468–20479, doi:10.1021/acs.est.4c06749.

40. Zhou, B.; Luo, Y.; Bi, H.; Zhang, N.; Ma, M.; Dong, Z.; Ji, N.; Zhang, S.; Wang, X.; Liu, Y.; et al. Amelioration of Nonalcoholic Fatty Liver Disease by Inhibiting the Deubiquitylating Enzyme RPN11. *Cell Metab.* 2024, 36, 2228–2244.e7, doi:10.1016/j.cmet.2024.07.014.

41. Baek, J.-H.; Kim, M.S.; Jung, H.R.; Hwang, M.-S.; Lee, C.-H.; Han, D.H.; Lee, Y.-H.; Yi, E.C.; Im, S.-S.; Hwang, I.; et al. Ablation of the Deubiquitinase USP15 Ameliorates Nonalcoholic Fatty Liver Disease and Nonalcoholic Steatohepatitis. *Exp. Mol. Med.* 2023, 55, 1520–1530, doi:10.1038/s12276-023-01036-7.

42. Kanayama, H.O.; Tamura, T.; Ugai, S.; Kagawa, S.; Tanahashi, N.; Yoshimura, T.; Tanaka, K.; Ichihara, A. Demonstration That a Human 26S Proteolytic Complex Consists of a Proteasome and Multiple Associated Protein Components and Hydrolyzes ATP and Ubiquitin-Ligated Proteins by Closely Linked Mechanisms. *Eur. J. Biochem.* 1992, 206, 567–578, doi:10.1111/j.1432-1033.1992.tb16961.x.

43. Sano, Y.; Furuta, A.; Setsuie, R.; Kikuchi, H.; Wang, Y.-L.; Sakurai, M.; Kwon, J.; Noda, M.; Wada, K. Photoreceptor Cell Apoptosis in the Retinal Degeneration of Uchl3-Deficient Mice. *Am. J. Pathol.* 2006, 169, 132–141, doi:10.2353/ajpath.2006.060085.

44. Andrés, C.M.C.; Pérez de la Lastra, J.M.; Andrés Juan, C.; Plou, F.J.; Pérez-Lebeña, E. Superoxide Anion Chemistry-Its Role at the Core of the Innate Immunity. *Int. J. Mol. Sci.* 2023, 24, doi:10.3390/ijms24031841.

45. Esposito, L.A.; Kokoszka, J.E.; Waymire, K.G.; Cottrell, B.; MacGregor, G.R.; Wallace, D.C. Mitochondrial Oxidative Stress in Mice Lacking the Glutathione Peroxidase-1 Gene. *Free Radic. Biol. Med.* 2000, 28, 754–766, doi:10.1016/s0891-5849(00)00161-1.

46. Esworthy, R.S.; Chu, F.F.; Paxton, R.J.; Akman, S.; Doroshow, J.H. Characterization and Partial Amino Acid Sequence of Human Plasma Glutathione Peroxidase. *Arch. Biochem. Biophys.* 1991, 286, 330–336, doi:10.1016/0003-9861(91)90048-n.

47. Sun, C.; Guo, Y.; Cong, P.; Tian, Y.; Gao, X. Liver Lipidomics Analysis Revealed the Novel Ameliorative Mechanisms of L-Carnitine on High-Fat Diet-Induced NAFLD Mice. *Nutrients* 2023, 15, doi:10.3390/nu15061359.

48. Semenov, A.L.; Gubareva, E.A.; Ermakova, E.D.; Dorofeeva, A.A.; Tumanyan, I.A.; Radetskaya, E.A.; Yurova, M.N.; Aboushanab, S.A.; Kanwugu, O.N.; Fedoros, E.I.; et al. Astaxanthin and Isoflavones Inhibit Benign Prostatic Hyperplasia in Rats by Reducing Oxidative Stress and Normalizing Ca/Mg Balance. *Plants* (Basel, Switzerland) 2021, 10, doi:10.3390/plants10122735.

49. Collins, A.; Møller, P.; Gajski, G.; Vodenková, S.; Abdulwahed, A.; Anderson, D.; Bankoglu, E.E.; Bonassi, S.; Boutet-Robinet, E.; Brunborg, G.; et al. Measuring DNA Modifications with the Comet Assay: A Compendium of Protocols. *Nat. Protoc.* 2023, 18, 929–989, doi:10.1038/s41596-022-00754-y.

50. Demichev, V.; Messner, C.B.; Vernardis, S.I.; Lilley, K.S.; Ralser, M. DIA-NN: Neural Networks and Interference Correction Enable Deep Proteome Coverage in High Throughput. *Nat. Methods* 2020, 17, 41–44, doi:10.1038/s41592-019-0638-x.
51. Virtanen, P.; Gommers, R.; Oliphant, T.E.; Haberland, M.; Reddy, T.; Cournapeau, D.; Burovski, E.; Peterson, P.; Weckesser, W.; Bright, J.; et al. SciPy 1.0: Fundamental Algorithms for Scientific Computing in Python. *Nat. Methods* 2020, 17, 261–272, doi:10.1038/s41592-019-0686-2.
52. Waskom, M. Seaborn: Statistical Data Visualization. *J. Open Source Softw.* 2021, 6, 3021, doi:10.21105/joss.03021.
53. Hunter, J.D. Matplotlib: A 2D Graphics Environment. *Comput. Sci. Eng.* 2007, 9, 90–95, doi:10.1109/MCSE.2007.55.
54. McKinney, W. Data Structures for Statistical Computing in Python. *Proc. 9th Python Sci. Conf.* 2010, 1, 56–61, doi:10.25080/majora-92bf1922-00a.
55. Friedjungová, M.; Vašata, D.; Balatsko, M.; Jiřina, M. Missing Features Reconstruction Using a Wasserstein Generative Adversarial Imputation Network. *Comput. Sci. – ICCS 2020 20th Int. Conf. Amsterdam, Netherlands, June 3–5, 2020, Proceedings, Part IV* 2020, 12140, 225–239.
56. Tonoyan, N.M.; Chagovets, V. V.; Starodubtseva, N.L.; Tokareva, A.O.; Chingin, K.; Kozachenko, I.F.; Adamyan, L. V.; Frankevich, V.E. Alterations in Lipid Profile upon Uterine Fibroids and Its Recurrence. *Sci. Rep.* 2021, 11, 11447, doi:10.1038/s41598-021-89859-0.
57. Kessner, D.; Chambers, M.; Burke, R.; Agus, D.; Mallick, P. ProteoWizard: Open Source Software for Rapid Proteomics Tools Development. *Bioinformatics* 2008, 24, 2534–2536, doi:10.1093/bioinformatics/btn323.
58. Goloborodko, A.A.; Levitsky, L.I.; Ivanov, M. V.; Gorshkov, M. V. Pyteomics--a Python Framework for Exploratory Data Analysis and Rapid Software Prototyping in Proteomics. *J. Am. Soc. Mass Spectrom.* 2013, 24, 301–304, doi:10.1007/s13361-012-0516-6.
59. Volikov, A.; Rukhovich, G.; Perminova, I. V. NOMspectra: An Open-Source Python Package for Processing High Resolution Mass Spectrometry Data on Natural Organic Matter. *J. Am. Soc. Mass Spectrom.* 2023, 34, 1524–1527, doi:10.1021/jasms.3c00003.
60. Zielinski, A.T.; Kourtchev, I.; Bortolini, C.; Fuller, S.J.; Giorio, C.; Popoola, O.A.M.; Bogialli, S.; Tapparo, A.; Jones, R.L.; Kalberer, M. A New Processing Scheme for Ultra-High Resolution Direct Infusion Mass Spectrometry Data. *Atmos. Environ.* 2018, 178, 129–139, doi:https://doi.org/10.1016/j.atmosenv.2018.01.034.
61. Kozhinov, A.N.; Zhurov, K.O.; Tsybin, Y.O. Iterative Method for Mass Spectra Recalibration via Empirical Estimation of the Mass Calibration Function for Fourier Transform Mass Spectrometry-Based Petroleomics. *Anal. Chem.* 2013, 85, 6437–6445, doi:10.1021/ac400972y.

Disclaimer/Publisher's Note: The statements, opinions and data contained in all publications are solely those of the individual author(s) and contributor(s) and not of MDPI and/or the editor(s). MDPI and/or the editor(s) disclaim responsibility for any injury to people or property resulting from any ideas, methods, instructions or products referred to in the content.